



**HAL**  
open science

## Assessment of the reliability of concrete evaluation by multi-physical inversion of NDT measurements – A probabilistic approach

Wafaa Abdallah, Zoubir-Mehdi Sbartai, Jacqueline Saliba, Sidi Mohammed Elachachi, Fadi Hage Chehade, Marwan Sadek

### ► To cite this version:

Wafaa Abdallah, Zoubir-Mehdi Sbartai, Jacqueline Saliba, Sidi Mohammed Elachachi, Fadi Hage Chehade, et al.. Assessment of the reliability of concrete evaluation by multi-physical inversion of NDT measurements – A probabilistic approach. *Construction and Building Materials*, 2021, 300, pp.124371. 10.1016/j.conbuildmat.2021.124371 . hal-03482897

**HAL Id: hal-03482897**

**<https://hal.science/hal-03482897>**

Submitted on 22 Aug 2023

**HAL** is a multi-disciplinary open access archive for the deposit and dissemination of scientific research documents, whether they are published or not. The documents may come from teaching and research institutions in France or abroad, or from public or private research centers.

L'archive ouverte pluridisciplinaire **HAL**, est destinée au dépôt et à la diffusion de documents scientifiques de niveau recherche, publiés ou non, émanant des établissements d'enseignement et de recherche français ou étrangers, des laboratoires publics ou privés.



Distributed under a Creative Commons Attribution - NonCommercial 4.0 International License

# Assessment of the reliability of concrete evaluation by multi-physical inversion of NDT measurements – A probabilistic approach

Wafaa Abdallah<sup>1,2</sup>, Zoubir-Mehdi Sbartai<sup>1</sup>, Jacqueline Saliba<sup>1</sup>, Sidi Mohammed Elachachi<sup>1</sup>, Fadi Hage Chehade<sup>2</sup>, Marwan Sadek<sup>2</sup>.

<sup>1</sup> I2M, UMR 5295, CNRS, Université de Bordeaux, Talence, France.

<sup>2</sup> EDST, Université Libanaise, Beyrouth, Liban.

Contact: [zoubir-mehdi.sbartai@u-bordeaux.fr](mailto:zoubir-mehdi.sbartai@u-bordeaux.fr)

## ABSTARCT

*The evaluation of the spatial variability of concrete properties is an important issue for a better diagnosis of reinforced concrete structures. The combination between destructive techniques and nondestructive techniques (NDT) is a common practice to establish relationships between concrete properties and NDT measurements. Concrete properties can then be estimated at each test location using the corresponding NDT values on the basis of the calibration and inversion of these relationships. However, NDT measurements include many sources of uncertainties that can lead to biased or even inaccurate estimation. Thus, the improvement of the reliability of this estimation requires to specify and control the principal influencing factors on these uncertainties. The main objective of this paper is to propose a calibration methodology of conversion models and to study the reliability of concrete properties assessment considering the effect of the number of measurements, the uncertainty of NDT measurements and the combination of NDT techniques. Three conversion models linking the ultrasonic pulse velocity, the electrical resistivity, and the dielectric permittivity to two physical concrete properties, the porosity and saturation degree, are considered. The results show that the inversion of the proposed analytical models enables an accurate*

evaluation of concrete properties. In addition, it has been shown that there is a minimal number of measurements needed for an efficient non-destructive evaluation of concrete properties considering their variabilities.

**Table A. Definitions of some terms presented in this study**

Name	Symbol	Definition
Non-destructive techniques	NDT	
Total number of numerical simulation	NS	
Measurement noise	$\xi$	Coefficient indicating the NDT measurement quality
Complete number of data	NM	-total number of measurement in calibration approach -total number of synthetic data set in inversion approach
Reduced number of data	NR	-number selected randomly from NM dataset
Root Mean Square Error	RMSE	-in calibration approach: $RMSE = \sqrt{\frac{\sum_{i=1}^{NR} (NDT_{(exp)} - NDT_{(mod)})^2}{NR}}$ (1) where " $NDT_{(exp)}$ " and " $NDT_{(mod)}$ " experimental and numerical NDT values respectively -in inversion approach: $RMSE = \sqrt{\frac{\sum_{i=1}^{NS} (\mu_{(after\ generation)} - \mu_{(after\ inversion)})^2}{NS}}$ (2) where " $\mu_{(after\ generation)}$ " and " $\mu_{(after\ inversion)}$ " the mean concrete properties (porosity or saturation degree) values after the random generation and after the inversion method respectively.
Fitting Error	FE	Error calculated for NDT values in fitting (calibration approach, using the formula (1) with n=NR from "NM".
Prediction Error	PE	Error calculated for NDT values in prediction approach, using the formula (1) with n=NR from "NM-NR".

## I. INTRODUCTION

Aging infrastructure and the resulting risks is an important issue nowadays. Many reinforced concrete structures are approaching the end of their design life and the number of structures that are considered to be structurally deficient is increasing. Thus, diagnosis of their state or the future state of new constructions for predictive maintenance is needed to ensure their safety and durability and prevent their failure. In this context, the implementation of NDT (Non-Destructive Techniques) to determine concrete properties and/or durability indicators is necessary to provide meaningful information about critical situations.

The combination of NDT measurements with optimal coring remains the most valuable way to ensure the reliability of concrete properties assessment with limited cost as reported by RILEM recommendations [1-4,41]. This NDT combination is an interesting tool to provide an efficient assessment of concrete properties that allows to reduce the disadvantages of destructive tests to preserves the desired level of structural performance [5-9]. However, one of the major challenges of structures diagnosis with NDT is the identification of conversion model that relates NDT measurements to concrete properties. Two model identification approaches are generally performed: regression approach where the identified model has a specific shape (linear or non-linear, power models) [10-12], and calibration approach where a proposed model of any shape is used and optimized for the best agreement with experimental data [13-15]. The methodology of assessing concrete properties in existing buildings consists in performing conversion models. Many conversion models between NDT observables and concrete properties have been proposed in the literature [16, 17]. However, none of the identified models represents a general model that predicts useable values of concrete properties due to measurements uncertainties and uncontrolled factors such as the exposure conditions and model parameters identification approach [18].

NDT techniques are influenced by many parameters. In fact, as an example, ultrasonic technique is sensitive to mechanical properties such as the strength which depends on porosity [18, 23, 24] and also to water saturation [23, 25]. Electrical resistivity and permittivity measurements are sensitive to porosity and water content [19-22]. The combination of complementary NDT can reduce the uncertainty regarding the evaluation of concrete properties as reported by [5, 17]. However, only statistical regressions of NDT have been used and limited results discussed combination of several NDT by taking into account uncertainty of measurements and evaluation methodology [26-28]. These influencing parameters are considered in this paper to evaluate the effectiveness of combining two or three NDT for the assessment of concrete properties as porosity and saturation degree.

Another issue must be considered concerning the reliability of the NDT measurements, namely the implemented assessment methodology and the determination of the spatial variability of concrete properties on site [29, 30]. The spatial variability of concrete results from the complexity and high heterogeneity of this material due to its constituent's variability such as the size, shape and nature of aggregates and from its exposure conditions such as the temperature and humidity [31, 32]. The quantification of spatial variability is based on the evaluation of the measurements dependence at different distances. The correlation length, or the distance from which the evaluated values are no longer correlated, can be determined [33]. The objective of this study is to propose an inversion method of the calibrated NDT models for a better assessment of concrete properties and their variabilities. First, experimental data is used for performing and testing the calibration of NDT models by considering different number of measurements. Then, since experimental data is limited, the inversion methodology is carried out using simulated dataset to analyze the capability of calibrated NDT models in assessing the concrete properties and their variabilities. The main advantage of using numerical simulations for calibration and inversion procedures is the ability to

modify any of the influencing factors for a better evaluation of its effect. Finally, a parametric study concerning the measurement uncertainty (i.e. measurement noise), the number of measurements (i.e. coring number) and the NDT combination type, is conducted and the results are presented and discussed.

## II. Assessing porosity and saturation degree using NDT methods

### II.1. NDT techniques and conversion models

Three analytical conversion models were considered to evaluate the porosity ( $\Phi$ ) and the saturation degree ( $S_r$ ) based on the permittivity, the electrical resistivity and the ultrasonic pulse velocity measurements.

The permittivity ( $\varepsilon$ ), obtained from the dielectric permittivity technique, was calculated using the Complex Refractive Index Model (CRIM) [34] which is a multiphasic model that takes into account the three phases of concrete:

$$\varepsilon^p = (1 - \Phi) * \varepsilon_{(s)}^p + \Phi * S_r * \varepsilon_{(w)}^p + \Phi * (1 - S_r) * \varepsilon_{(a)}^p \quad (1)$$

Where ( $\varepsilon$ ) is the permittivity of the mixture (without unit) which can be measured by capacitive method or Ground Penetrating Radar (GPR) [23, 35, 36],  $\varepsilon_{(s)}$  is the permittivity of the solid phase (aggregates and cement paste),  $\varepsilon_{(a)}$  is the permittivity of the gas phase ( $\varepsilon_{(a)} = 1$  [34]),  $\varepsilon_{(w)}$  is the permittivity of the liquid phase ( $\varepsilon_{(w)} = 75$  according to [17]) and  $p$  is a constant coefficient.

Regarding electrical resistivity technique, the electrical resistivity ( $\rho$ ) was determined based on Archie's law [37]:

$$\rho = a * \rho_w * \Phi^{-m} * S_r^{-n} \quad (2)$$

Where  $\rho_w$  is the resistivity of the interstitial water ( $\rho_w = 1 \Omega.m$ ),  $a$ ,  $m$  and  $n$  are material-dependent parameters identified based on experimental data.

The Ultrasonic Pulse Velocity (*UPV*) is calculated based on the fraction of concrete components:

$$UPV^r = f_{ag} * UPV_{(ag)}^r + (1 - f_{ag} - \Phi) * UPV_{(s)}^r + \Phi * S_r * UPV_{(w)}^r + \Phi * (1 - S_r) * UPV_{(a)}^r \quad (3)$$

Where *UPV*, *UPV*<sub>(ag)</sub>, *UPV*<sub>(s)</sub>, *UPV*<sub>(w)</sub> and *UPV*<sub>(a)</sub> are the *UPV* of concrete, aggregates, solid phase of cement paste, water and air respectively. *f*<sub>ag</sub> is the volume fraction of aggregates and *r* is a constant coefficient. *UPV*<sub>(w)</sub> and *UPV*<sub>(a)</sub> are taken equal to 1500 and 350 m/s respectively [38, 39].

## II.2. Calibration of conversion models

The calibration process of the selected conversion models is the main first step to estimate concrete properties. The calibration consists in determining the coefficients of these models that minimize the error between experimental and numerical models. Experimental data is obtained from a part of the large experimental campaign realized in the context of a national French project SENSO [23]. Tests were carried out on slabs of 50 cm x 25 cm x 12 cm where six different mixtures with round siliceous aggregates (0–14 mm) with different water to cement ratio (*w/c*) have been used [23]. NDT measurements have been carried out on all samples (samples for each mixture as presented in table 1). Porosity and compressive strength (at 28 days) were determined by destructive tests following the recommendations of AFPC-AFREM [23]. Three series of tests for different saturation degrees *S<sub>r</sub>* are considered: The first one corresponds to an oven-drying (*S<sub>r</sub>* =0%) of samples up to constant weight (in this case, the measurement is affected mainly by the porosity). After that the second series consists of saturated condition (*S<sub>r</sub>* =100%) by a capillary absorption of samples up to constant weight. At last, different intermediate saturation degrees (40%, 60% and 80%) are concerned for the

remaining samples in each mixture to evaluate the effect of different controlled saturation degrees.

The data set of each concrete mixture is presented in table (1). The mean compressive strength ( $f_{cm}$ ) and the mean porosity ( $\Phi_m$ ) of concrete are also shown. Three samples were investigated for each mixture in order to evaluate the variability of NDT measurements [23].

The range of variation of  $UPV$ ,  $\rho$  and  $\varepsilon$  in function of  $S_r$  in each mixture is detailed in table (1).

**Table 1. Summary of the experimental results with six concrete mixtures [23]**

N° Dataset	W/C	$f_{cm}$ (MPa)	$S_r$ (%)	$\Phi_m$ (%)	UPV (m/s)*	$\varepsilon^*$	$\rho$ ( $\Omega.m$ )*
1	0.47	55.6	0 - 100	14.3	3641-4928	6.07 -10.69	156-3260
2	0.59	46.0	0 - 100	15.5	3683-4747	5.79-10.07	115-4616
3	0.57	43.3	0 - 100	15.2	4164-4769	5.83-9.63	99-2083
4	0.63	44.3	0 - 100	15.9	4047-4755	5.72-9.12	121-2308
5	0.9	27.5	0 - 100	18.1	3882-4403	5.75-9.86	85-3316
6	0.62	44.0	0 - 100	16.0	3949-4703	5.95-10.17	106-2795

\*: range of values

### **II.2.1. NDT models calibration**

Numerical simulations are implemented to develop the calibration procedure and its validation since they allow studying the effect of some factors such as the number of measurements and the measurement uncertainty on this calibration.

Figure (1) presents the flowchart of calibration approach. The different steps of the adopted approach are:



-Step 1: The experimental data set of  $S_r$  and  $\Phi$  with the corresponding  $UPV$ ,  $\rho$  and  $\varepsilon$  is collected;

-Step 2: In order to simulate the repeatability of the NDT measurements, a noise ' $\xi$ ' was generated randomly and added to the values considering a Gaussian random variable with a mean  $\mu_\xi$  of 0% and a coefficient of variation  $COV_\xi$  of 0%, 2% or 5%. Hence, the experimental NDT values correspond to:  $NDT_{i,noisy} = (1 + \xi_i) \times NDT_{i, measured}$ , where  $i$  is the index from 1 to the complete number of data (NM=100).

-Step 3: As part of an approach that is intended to be sufficiently practical, a reduced number of measures (NR) is selected randomly among the complete data collected in step 1; Then, the model's parameters (equations (1), (2) and (3)) are identified using NR. The identified parameters are:

- $UPV_{(s)}$ ,  $UPV_{(ag)}$  and  $r$  for the  $UPV$  model;
- $\varepsilon_{(s)}$  and  $p$  for the permittivity model ;
- $a$ ,  $m$  and  $n$  for the resistivity model.

Those parameters are determined based on the minimization of the root mean square error RMSE (equation (4)) between the NR of experimental and estimated NDT parameters by the corresponding model (equations (1), (2) and (3)).

$$RMSE = \sqrt{\frac{\sum_{i=1}^{NR} (NDT_{(exp)} - NDT_{(mod)})^2}{NR}} \quad (4)$$

-Step 4: The calibration is tested by choosing randomly the remaining values "NM-NR" not used in the calibration step (step3). Estimated NDT values are predicted using the conversion models with parameters identified in step 3 and, then, the RMSE is calculated again between experimental and estimated NDT values.

Because of the random generation of measurement noise and the random selection of NR, this numerical process was repeated to obtain a simulation number (NS) of 250. This selected NS presents a compromise to produce fastly and efficiently representative results. At the end, two types of RMSE values are obtained. The first, regarding NR for the identification step (step 3), quantifies the fitting error (FE). The second, obtained while testing the calibration with “NM-NR” (step 4), quantifies the Prediction Error (PE). The PE allows to quantify the capacity of this calibration to predict the exact NDT values with taking into account the uncertainty and number of measurements [5, 28].

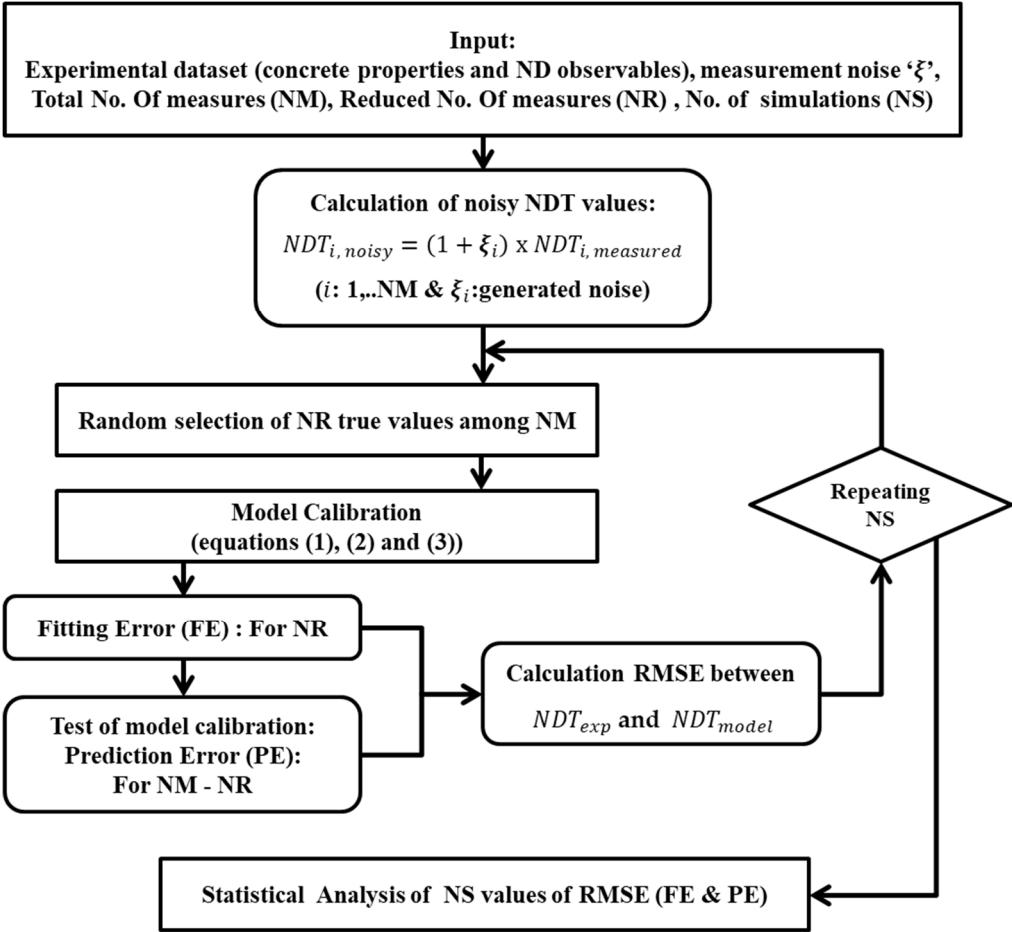


Figure 1. Flowchart of calibration approach

Table (2) summarizes the average and standard deviation values of 250 simulations for the calibrated parameters with  $\xi=0\%$  and a dataset randomly reduced to 20 measurements from NM. The value of these parameters is within the allowed margin:

- $0.5 < a < 3$  ;  $1.3 < m < 2.5$  and  $2 < n < 3$  [37] for the resistivity model ;
- $4 < \varepsilon_{(s)} < 8$  and  $p = 0.5$  [17,34] for the permittivity model ;

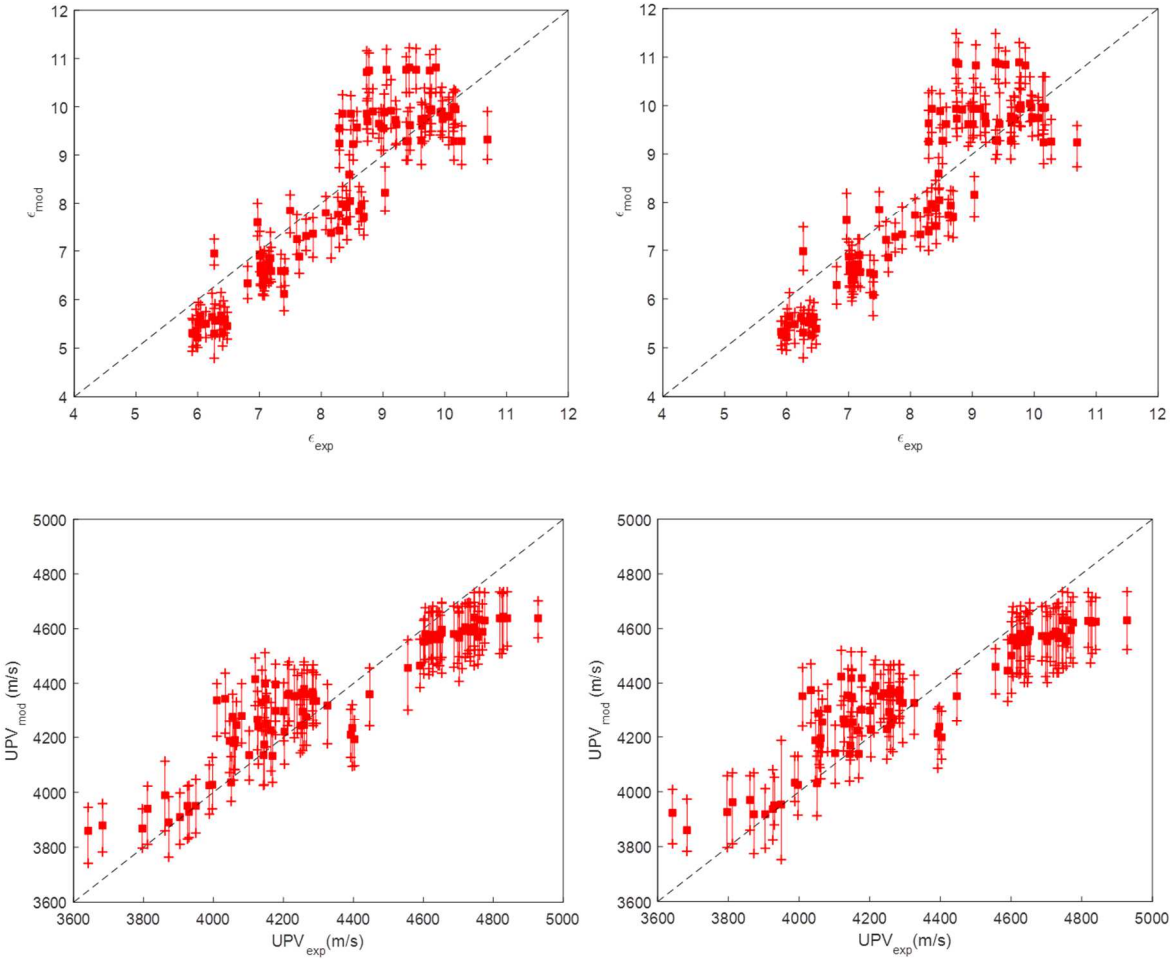
and for the  $UPV$  model, the velocity in the solid phase of cement paste  $UPV_{(s)}$  and in the aggregates  $UPV_{(ag)}$  are in the order of  $5000 \text{ m/s}$  [17]. Based on these first results and the literature review, the corresponding conversion models can be considered validated with these identified values.

**Table 2. Synthesis of models calibration: case of NR=20 and  $\xi = 0\%$**

<b>Coefficients of resistivity model</b>			
$a$	$m$	$n$	RMSE ( $\Omega.m$ )
$1.97 \pm 0.71$	$2.18 \pm 0.24$	$2.78 \pm 0.26$	222.64
<b>Coefficients of permittivity model</b>			
$\varepsilon_{(s)}$	$p$	RMSE	
$4.44 \pm 0.14$	0.50	0.74	
<b>Coefficient of UPV model</b>			
$UPV_{(s)}(m/s)$	$UPV_{(ag)}(m/s)$	$r$	RMSE ( $m/s$ )
$5033.36 \pm 153.96$	$5213.36 \pm 64.81$	0.50	218.40

Figure 2 presents the estimated  $UPV$ ,  $\rho$  and  $\varepsilon$  numerical values versus the experimental ones for the 250 sets obtained during the calibration and the validation steps with  $\xi=0\%$ . Each set corresponds to NR=20 measures selected randomly from NM=100 and from NM-NR=80. The evolution of the estimated NDT values gravitates around the bisector of the experimental ones

not only at fitting stage as expected, but also at the validation stage indicating that the calibrated NDT models can be validated with another set of measures not used in the calibration process. As it is unpractical to show the results for all the tried cases of NR, it is important to mention that the case of NR=20 is chosen here as an example to show the results of the calibration approach. To deepen the analysis, the effect of NR and  $\xi$  are presented in the following section.



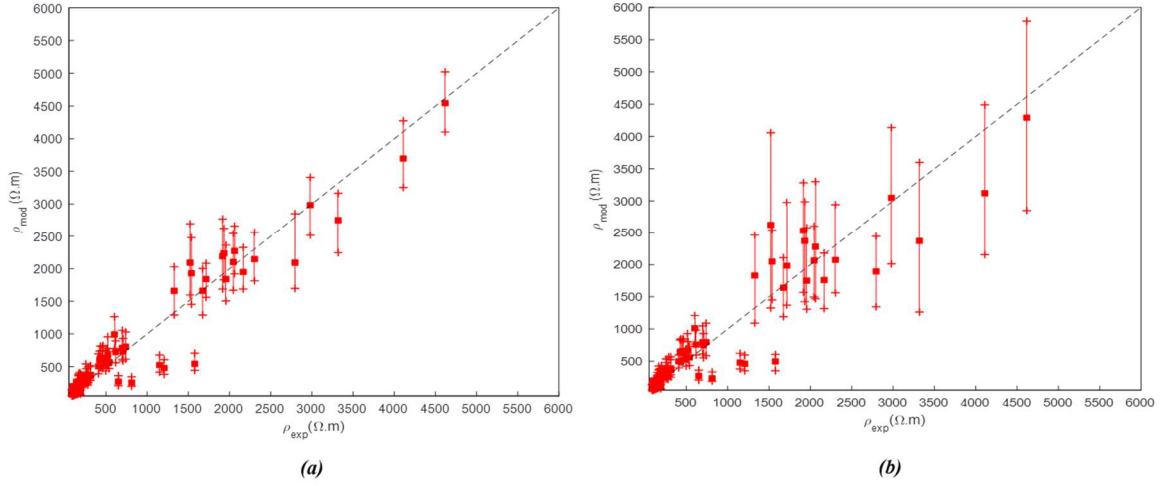


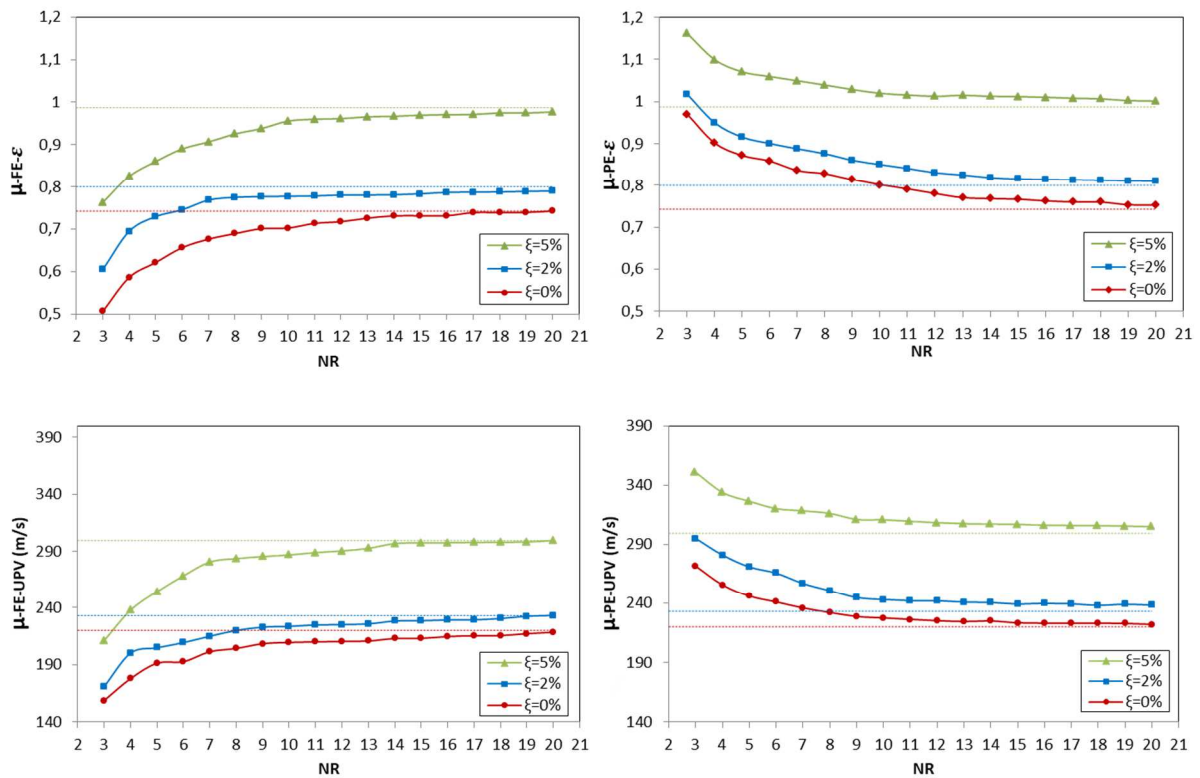
**Figure 2. Estimated  $\varepsilon$ ,  $UPV$  and  $\rho$  values versus the experimental ones obtained during (a) calibration and (b) validation when  $NR = 20$  and  $\xi=0\%$ .**

### **II.2.2. Effect of measurements number**

Figures 3 and 4 show the evolution of the mean " $\mu$ " and standard deviation " $\sigma$ " of RMSE of each NDT technique in function of NR which varies from 3 to 20. The mean fitting error (FE) of each NDT increases with NR. This could be explained by the increased number of points to be fitted with NR while using models having a fixed number of parameters. An inverse tendency has been observed at the prediction stage since the models provide a better estimation when the number of measurements increases. Consequently, by increasing NR, the standard deviations of FE and PE decrease as shown in figure 4. On the other hand, PE and FE converge with the increase of NR and almost coincide with  $NR = 20$  for any added measurement noise. It's not sure that when the fitted model has a good fitting, the prediction will be the same [5, 28]. In fact, for small NR values ( $NR < 9$ ), PE can be more than at least 1.5 times the FE value for each NDT regardless the measurement noise value (figure 3). For  $NR \geq 11$ , a stabilization of PE and FE is observed. For example, with  $\xi=2\%$ , they are around 235 m/s for RMSE with  $UPV$ , 0.8 for RMSE with  $\varepsilon$  and 235  $\Omega.m$  for RMSE with  $\rho$ . The

prediction does not improve by further increase of NR. Thus, a value of NR=11 is sufficient regarding the fitting and prediction in this case. In addition, low measurement quality (i.e. high  $\xi$ ) will reduce the fitting and prediction performance since the mean and the standard deviation of FE and PE increase with the noise for *UPV* and  $\varepsilon$  except for  $\rho$  where the effect of  $\xi$  is negligible.

It is important to mention here that the performed calibration must be satisfied in the presence of conflicting objectives: (a) increase NR for model calibration to consolidate the stability of the conversion model, (b) increase NM and thus “NM-NR” to validate the model, while (c) preferably restricting NM for economic goals. To provide an answer, numerical simulations have been used for the calibration methodology in order to analyze efficiently the effect of NR and NM without any supplementary cost.



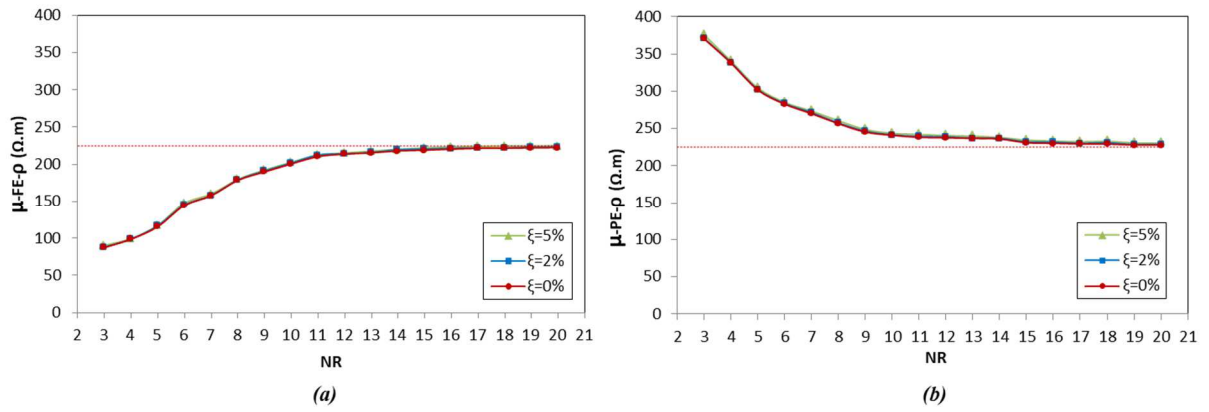
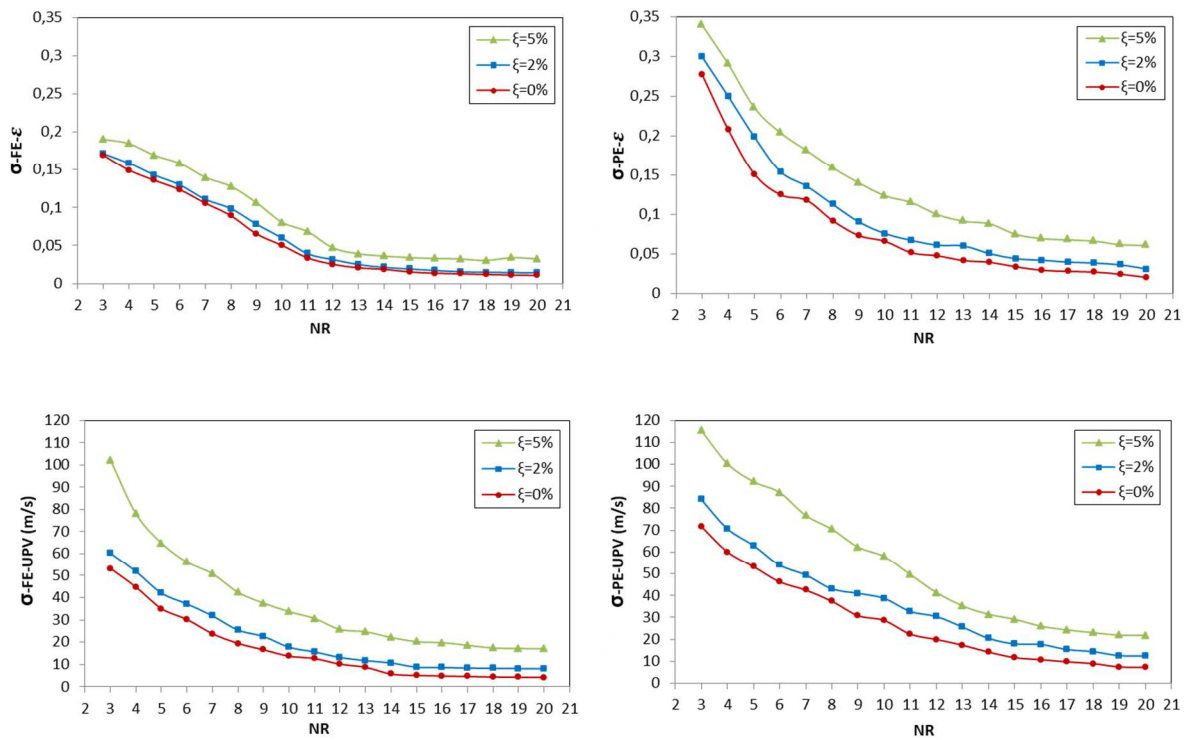


Figure 3. Variation of the mean value " $\mu$ " of (a) FE and (b) PE for  $\varepsilon$ , UPV and  $\rho$  in function of NR



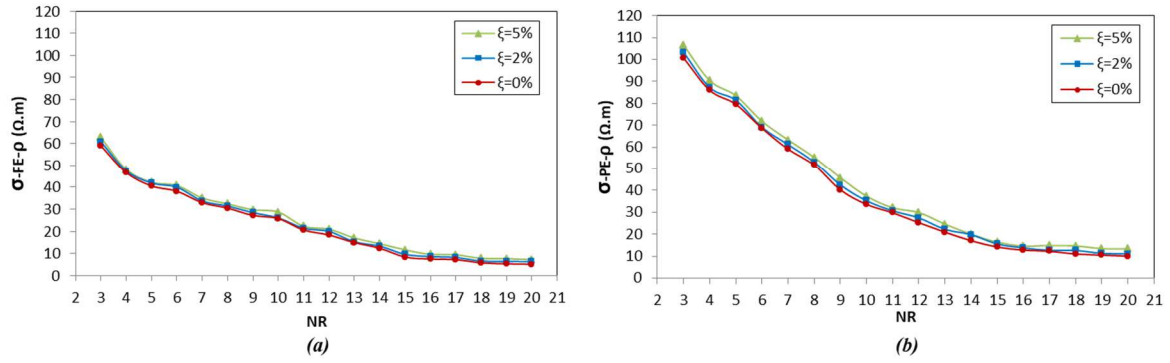


Figure 4. Variation of the standard deviation " $\sigma$ " of (a) FE and (b) PE for  $\epsilon$ ,  $UPV$  and  $\rho$  in function of NR

### III. Models inversion methodology for concrete properties evaluation by NDT

After the calibration process of conversion models obtained from the relations between destructive and non-destructive tests results, the inversion methodology of these models is the second essential step in investigation program for concrete properties evaluation. In real investigation programs as expressed in [41], the optimal assessment of concrete properties in a structure is based on extracting a limited number of cores NR based on NDT measurements carried out in the test locations NM [5, 28]. To represent the real practice, a numerical approach is simulated to evaluate the concrete properties by NDT techniques and perform a parametric study of the influencing factors that affect the reliability of this evaluation.

The effect of varying different factors such as the measurement noise, the reduced number of cores and the effect of combining two or three NDT techniques on concrete properties assessment quality has been studied using Monte-Carlo simulations. The considered case study is a 2D square slab with side of 10 m. Figure 5 presents the flowchart of the followed inversion approach. Different steps can be distinguished:

- The first step consists in creating a synthetic data set of  $\Phi$  and  $S_r$ . The mean and the standard deviation of  $\Phi$  and  $S_r$  are used as a reference for the estimated values after inversion of NDT



models. Synthetic NDT values are then calculated in each mesh element (i.e. test location) using the three calibrated conversion models (§ II.2) based on the generated values of  $\Phi$  and  $S_r$ . The total number of generated values NM is equal to 100. Typical distribution maps of  $\Phi$  and  $S_r$  are presented in Figure 6. The mean and standard deviation of  $\Phi$  and  $S_r$  are in the practical range of  $16.1 \pm 2.28\%$  and  $52.6 \pm 5.5\%$  respectively. The range of variation of NDT observables in function of the generated values of  $\Phi$  and  $S_r$  are respectively [5.57-8.48] for  $\varepsilon$ , [3930 - 4564 m/s] for  $UPV$  and [168 - 2826  $\Omega.m$ ] for  $\rho$  (figure 7).

-The second step consists in reducing the size of the synthetic dataset in each simulation. In other words, a random number of cores NR is selected among the NM synthetic test locations. To take into account the repeatability of NDT measurements, noise was generated by assuming a Gaussian distribution ( $\mu_\xi = 0\%$  and  $COV_\xi = 0,2\%$  or  $5\%$ ) for each NDT parameter.

The inversion method includes four types of NDT combinations from three variables: ( $UPV, \varepsilon, \rho$ ), ( $UPV, \rho$ ), ( $UPV, \varepsilon$ ) and ( $\varepsilon, \rho$ ). As, the equations relating the NDT with  $\Phi$  and  $S_r$  are multiple non-linear equations with different shapes (equations (1), (2) and (3)), the inversion is carried out by the Gauss-Newton optimization method [40]. Consequently, for each NR and in each simulation, the inversion of the corresponding models was performed in a same numerical optimization process and allowed to calculate simultaneously the estimated concrete properties values  $\Phi$  and  $S_r$ .

- The mean and the standard deviation of  $\Phi$  and  $S_r$  obtained with the inversion method are calculated. These estimated values are then compared to the reference values by means of RMSE error function. Because of the random character of the numerical process (random generation of noise and cores) and in order to have meaningful outputs, several simulations have been generated for each NR data set. The process was repeated 250 times, for which the convergence and stability of outputs are ascertained [1].

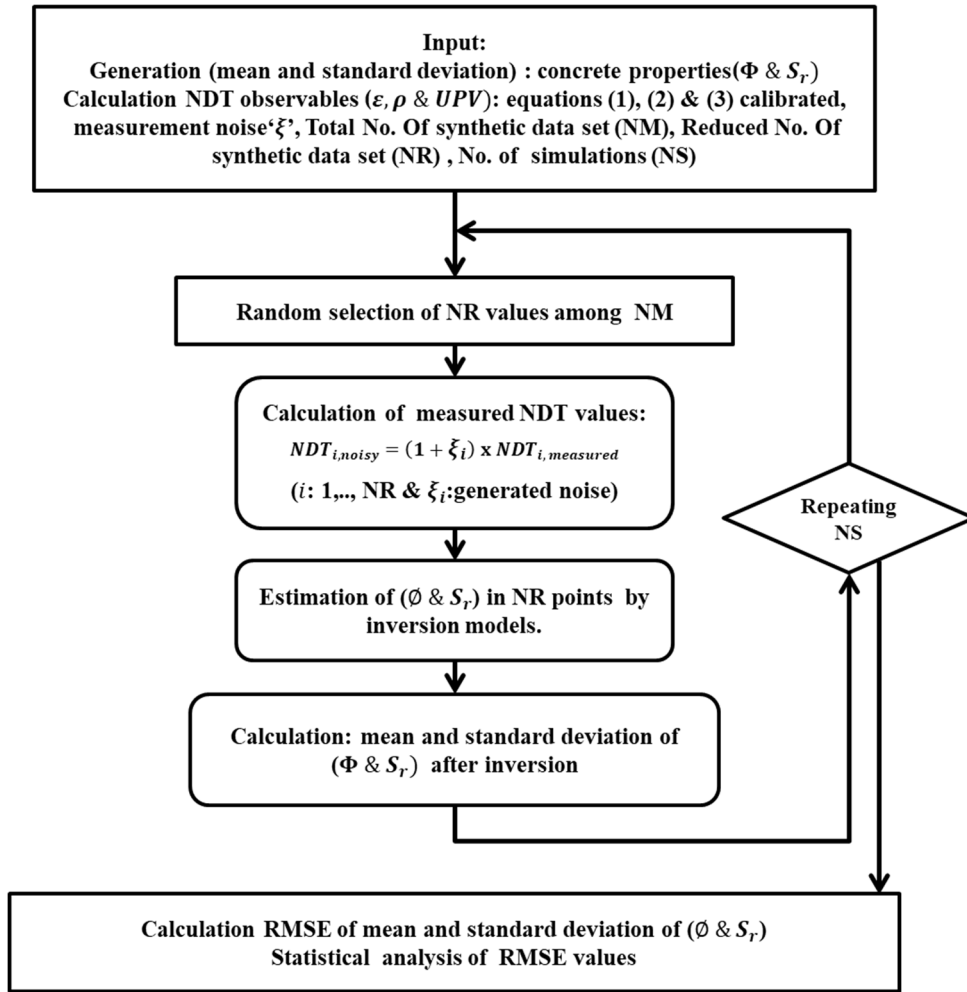


Figure 5. Flowchart of multi-physical NDT inversion approach

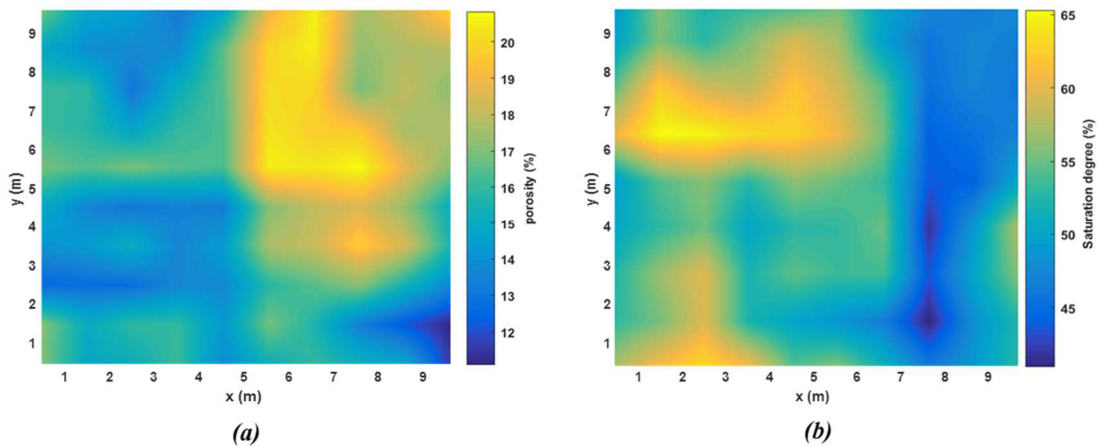
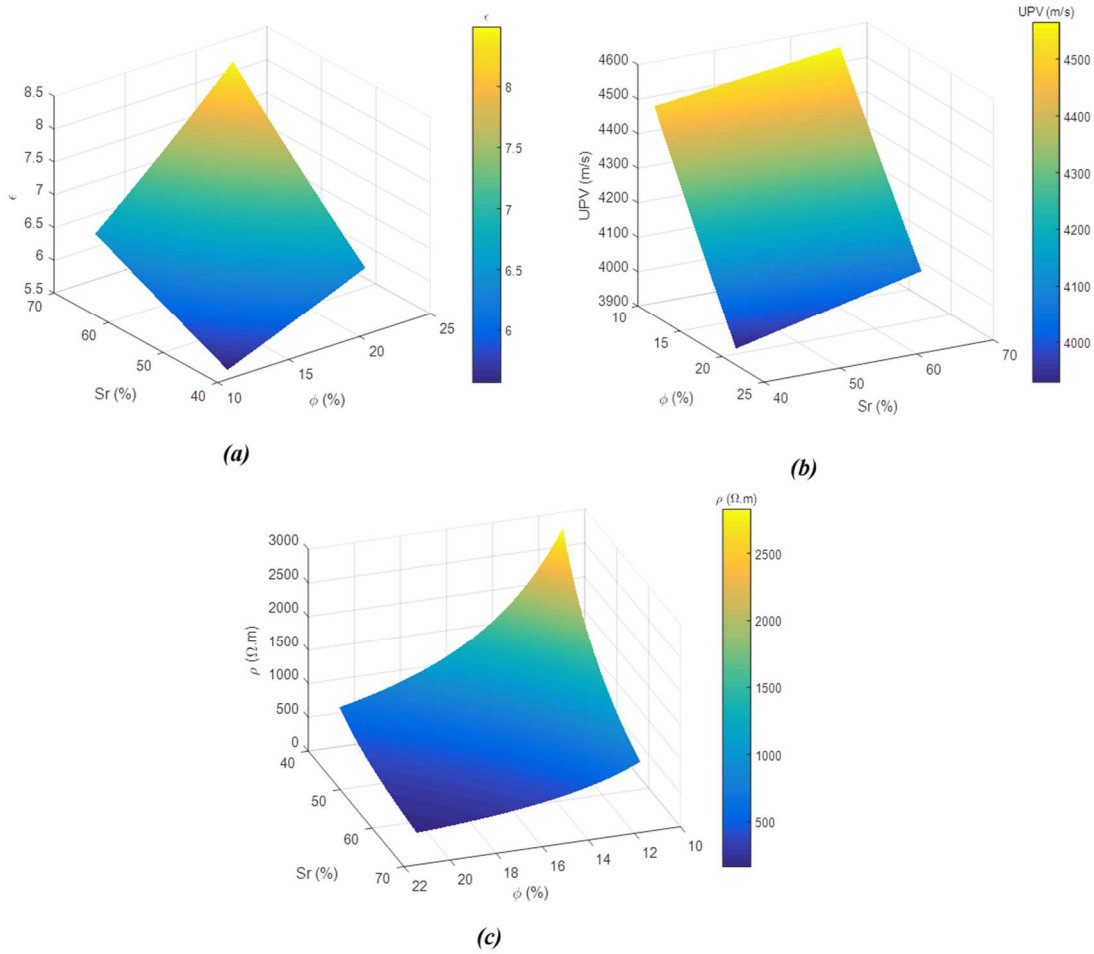


Figure 6. Distribution maps of the random generation of (a)  $\Phi$  and (b)  $S_r$



**Figure 7. Evolution of (a)  $\varepsilon$  (b) UPV and (c)  $\rho$  in function of the generated values of  $\Phi$  and  $S_r$ .**

To learn more if the proposed methodology can be adopted to assess the concrete properties and their spatial variability, the effect of NR and  $\xi$  on the RMSE values for  $\mu_\Phi$  and  $\sigma_\Phi$  is studied with the different NDT combination configuration (Figure 8). The general features are identical for all type of NDT combination with RMSE values that decrease with the increase of NR and the decrease of  $\xi$  except for the  $(\varepsilon, \rho)$  combination where the effect of  $\xi$  is low. Thus, by increasing NR and the measurement quality, the conversion models provide a better estimation of  $\Phi$ . It can be noted that, the accuracy of  $\Phi$  estimation using  $(\varepsilon, \rho)$  combination is clearly affected by a high measurement noise ( $\xi > 10\%$ ). However, as this case is rarely

founded, it is not presented in this paper. On the other hand, RMSE values are almost identical for  $(UPV, \varepsilon, \rho)$ ,  $(UPV, \rho)$  and  $(UPV, \varepsilon)$  combinations except for RMSE values on  $\sigma_\Phi$  using the  $(UPV, \varepsilon)$  combination when  $\xi=5\%$  (figure 8c). Consequently, as an example, same NR is needed by these combinations to have about 1% of RMSE for  $\mu_\Phi$  in each considered measurement noise (figure 9a). This figure shows also that by increasing  $\xi$ , the selected number of cores must be higher in inversion technique using these types of combinations. In figure 8, RMSE values are the smallest for  $\mu_\Phi$  and  $\sigma_\Phi$  with these combinations mainly when  $\xi=0\%$  or  $2\%$ . Thus, the presence of *UPV* with low and average quality has the most important influence on the assessment approach in comparison to the other NDT observables. Since  $(\varepsilon, \rho)$  combination is slowly affected by the noise, this type of combination (i.e. in a lack of *UPV*) seems effective to evaluate the mean and standard deviation of  $\Phi$  for a high measurement noise ( $\xi=5\%$ ) as the RMSE values are the smallest ones (figure 8c). For example, for any measurement noise,  $NR = 8$  is sufficient to have a RMSE value of 1% for  $\mu_\Phi$  (figure 9a). At last, it is essential to mention here, that a convergence of RMSE values of  $\mu_\Phi$  and  $\sigma_\Phi$  is observed with 13 cores, regardless of the combination type and measurement quality.

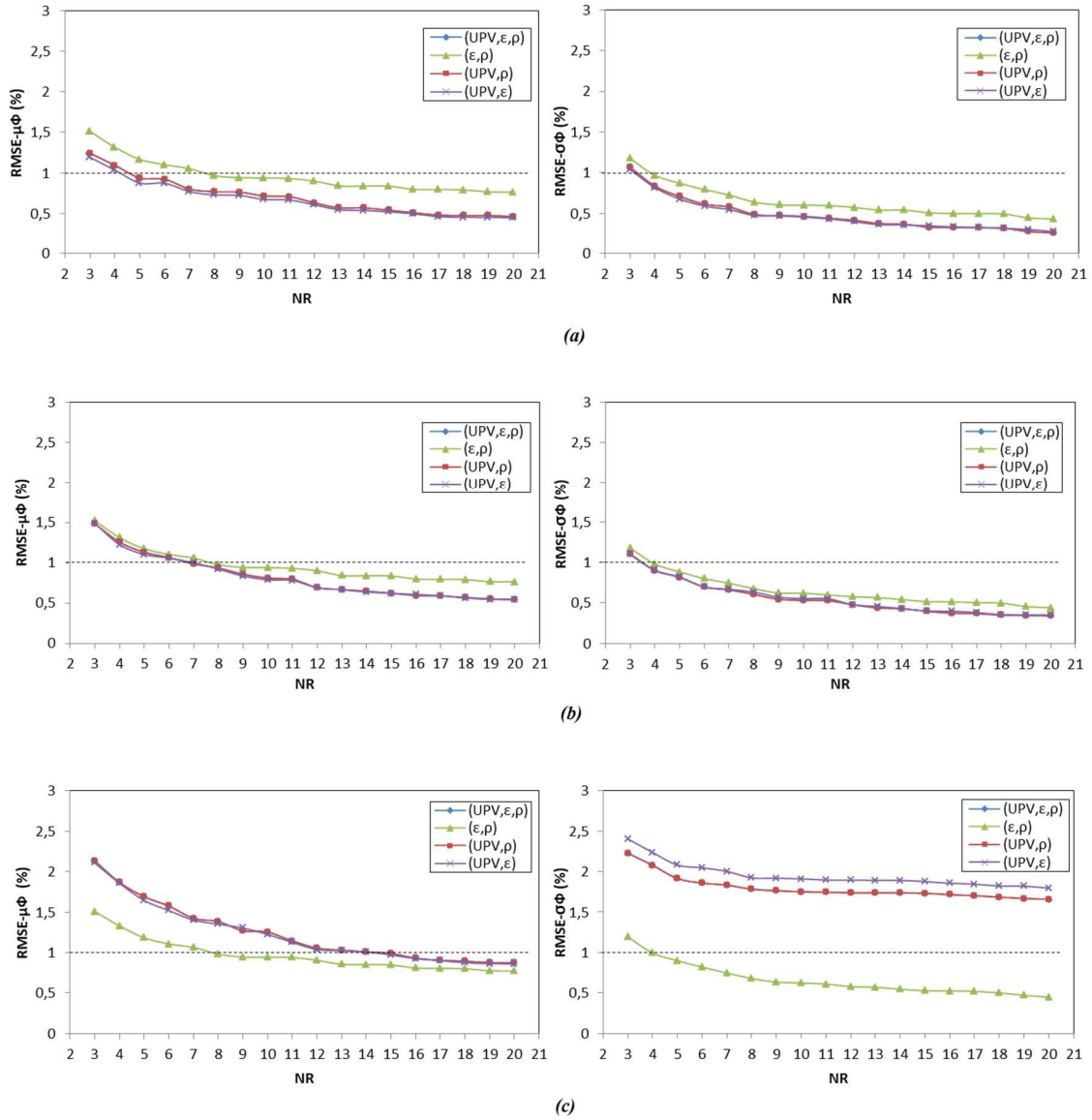


**Figure 8.** Variation of RMSE for  $\mu_\phi$  and  $\sigma_\phi$  in function of NR with different inversion combination type and different measurement noise (a) ( $\xi=0\%$ ) (b) ( $\xi=2\%$ ) and (c) ( $\xi=5\%$ )

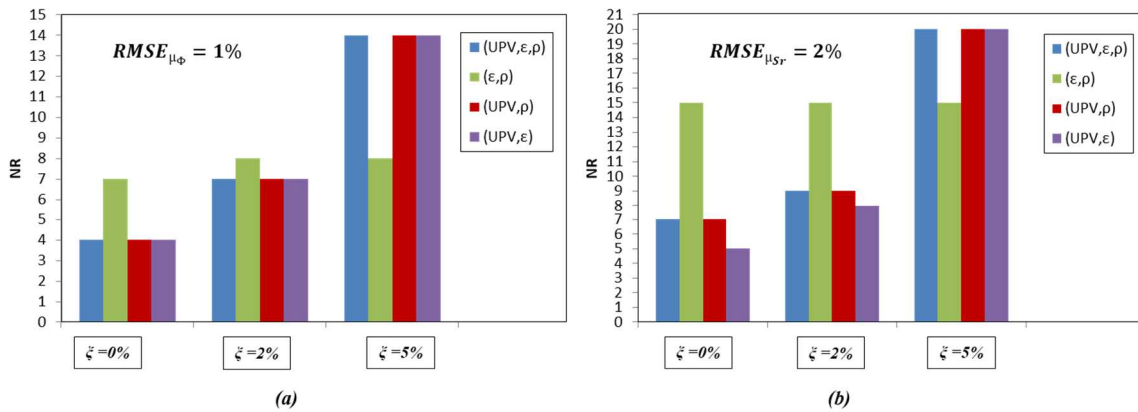


**Figure 9. Distribution of NR in function of the measurement noise where (a)  $RMSE_{\mu_{\phi}} = 1\%$  and (b)  $RMSE_{\mu_{S_r}} = 2\%$  for different inversion combination types.**

Figure 10a illustrates the cumulative distribution function of estimated mean porosity for different inversion combination configuration in the case of NR = 13 and  $\xi=2\%$ . Each distribution function corresponds to the 250 set values of mean porosity corresponding to the 13 measurements points. The comparison between the mean of each cumulative distribution function and the reference value of mean porosity emphasizes that the  $(\epsilon, \rho)$  combination overestimates the mean of porosity, while the other combinations are better in this estimation, since the difference between the estimated and the reference mean value of  $\Phi$  (after the random generation) is almost negligible.

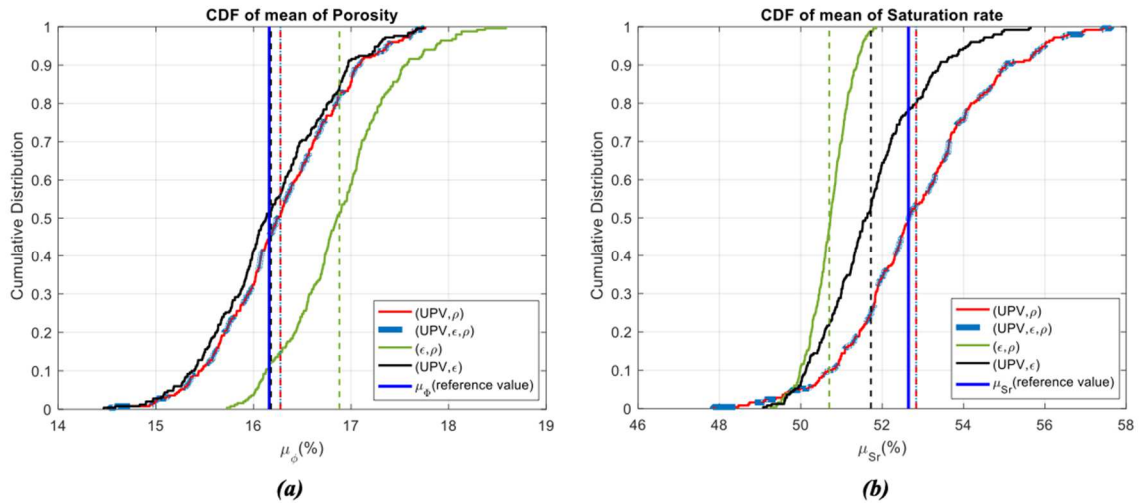


**Figure 10. Cumulative distribution function of the estimated mean of (a)  $\Phi$  and (b)  $S_r$  for different combination configuration in comparison with their reference values - case of NR = 13 and  $\xi = 2\%$ .**

The analysis of RMSE for  $\mu_{S_r}$  and  $\sigma_{S_r}$  has the same analogy as that of  $\Phi$ . Table 4 summarizes the RMSE values with different NR. An example about how NR evolves considering  $\xi$  for different combination type to have  $RMSE_{\mu_{S_r}} = 2\%$  is presented in figure 9b. Figure 10b shows also one case about the efficiency of  $S_r$  estimation by  $(UPV, \epsilon, \rho)$ ,  $(UPV, \rho)$  and  $(UPV, \epsilon)$

combinations in the same way adopted to analyze their efficiency in  $\Phi$  estimation (figure 10a).

As mentioned before, the efficiency of NDT combination for the assessment of concrete properties and their spatial variability depends on NR, NDT measurement repeatability, and the combination configuration of two or more NDT measurements. Thus, a balance between the cost and the evaluation efficiency must be sought in practical studies by optimizing the influencing parameters. In this part of the study, it can be concluded that, with  $\xi=2\%$  and NR=13, a combination of  $UPV, \varepsilon$  and  $\rho$  measurement can be appropriate to have a reliable assessment of  $\Phi$  and  $S_r$  and their variability with RMSE in an acceptable range (not more than 0.5% for the mean and standard deviation of  $\Phi$ , and 2% for the mean and standard deviation of  $S_r$ ).

**Table 4. RMSE for  $\mu_{S_r}$  and  $\sigma_{S_r}$  with different inversion combination type (a) ( $UPV, \varepsilon, \rho$ ), (b) ( $UPV, \rho$ ), (c) ( $UPV, \varepsilon$ ) and (d) ( $\varepsilon, \rho$ ) resulting from 250 simulations with NR = 3, 5, 7, 9, 12, 15 and 20.**

RMSE (%)		( $UPV, \varepsilon, \rho$ )		( $UPV, \rho$ )		( $UPV, \varepsilon$ )		( $\varepsilon, \rho$ )	
		$\mu_{S_r}(\%)$	$\sigma_{S_r}(\%)$	$\mu_{S_r}(\%)$	$\sigma_{S_r}(\%)$	$\mu_{S_r}(\%)$	$\sigma_{S_r}(\%)$	$\mu_{S_r}(\%)$	$\sigma_{S_r}(\%)$
NR=3	$\xi=0\%$	2.39	2.34	2.39	2.34	2.27	2.73	2.77	4.01
	$\xi=2\%$	3.28	2.92	3.28	2.92	3.22	2.96	2.80	4.02
	$\xi=5\%$	4.71	7.73	4.71	7.73	4.93	7.41	2.98	4.03
NR=5	$\xi=0\%$	2.25	1.77	2.25	1.77	2.01	2.02	2.29	3.72
	$\xi=2\%$	3.02	2.39	3.02	2.39	2.27	2.46	2.29	3.73
	$\xi=5\%$	4.02	7.13	4.02	7.13	4.73	6.96	2.30	3.74
NR=7	$\xi=0\%$	2.05	1.47	2.05	1.47	1.77	1.76	2.25	3.64
	$\xi=2\%$	2.64	2.27	2.64	2.27	2.04	1.87	2.27	3.65
	$\xi=5\%$	3.51	6.68	3.51	6.68	3.53	6.20	2.28	3.66
NR=9	$\xi=0\%$	1.76	1.18	1.76	1.18	1.63	1.62	2.10	3.57
	$\xi=2\%$	2.04	1.81	2.04	1.81	1.93	1.71	2.12	3.61
	$\xi=5\%$	2.95	6.54	2.95	6.54	2.90	6.18	2.13	3.63
NR=12	$\xi=0\%$	1.61	0.99	1.61	0.99	1.55	1.48	2.09	3.47
	$\xi=2\%$	1.95	1.67	1.95	1.67	1.79	1.53	2.11	3.49
	$\xi=5\%$	2.39	6.35	2.39	6.35	2.60	5.84	2.12	3.50
NR=15	$\xi=0\%$	1.31	0.87	1.31	0.87	1.28	1.35	2.06	3.43
	$\xi=2\%$	1.63	1.64	1.63	1.64	1.59	1.38	2.07	3.45
	$\xi=5\%$	2.36	6.08	2.36	6.08	2.52	4.86	2.08	3.47

NR=20	$\xi=0\%$	1.02	0.70	1.02	0.70	1.04	1.14	1.63	2.42
	$\xi=2\%$	1.41	1.41	1.41	1.41	1.38	1.28	1.64	2.43
	$\xi=5\%$	2.03	5.41	2.03	5.41	2.01	3.81	1.65	2.44

#### IV. CONCLUSIONS

The efficiency of calibration and inversion approaches for predicting concrete properties and their variability with NDT have been evaluated in this paper. Three conversion models relating  $UPV$ ,  $\rho$  and  $\varepsilon$  to  $\Phi$  and  $S_r$  have been implemented. First, the parameters of the conversion models have been identified based on minimizing the error, in terms of RMSE, between experimental and estimated values of NDT. The cloud of estimated NDT values is in the zone of bisector of the experimental values. The identification approach depends on the measurements number and the noise of NDT measurements (repeatability). RMSE values decreased with the increase of measurements number and the decrease of measurements noise.

Secondly, the capability of the calibrated conversion models to assess concrete properties has been evaluated considering different NDT combinations. Synthetic simulations have been used to better evaluate the influencing factors on concrete properties determination and their variability. The difference between the mean and standard deviation of  $\Phi$  and  $S_r$  before and after NDT models inversion has been evaluated and acceptable values have been obtained. Maximum values of RMSE were around 1% and 2% respectively for the mean and standard deviation of  $\Phi$ , and around 2.3% and 3.4% respectively for the mean and standard deviation of  $S_r$ . RMSE decreases with the increase of the number of cores and the decrease of the noise except for  $(\varepsilon, \rho)$  combination where the effect of the noise was negligible. The results show that in the case of this study the added-value of increasing the number of cores beyond 10 is not needed.  $(UPV, \varepsilon, \rho)$ ,  $(UPV, \rho)$  and  $(UPV, \varepsilon)$  were the most effective combinations to assess in the same time  $\Phi$  and  $S_r$  considering the number of measurements and noise.



The proposed approach can be an extension of the proposed RILEM recommendations [41] which is a general methodology of concrete strength evaluation on-site. In this study we added the fact that physical models can be used for NDT calibration by taking into account NDT uncertainty. In addition, three NDT can be combined for the evaluation of at least two concrete properties (porosity and saturation degree) in the case of this study. We demonstrated that, the proposed models can be calibrated and inverted (resolved) in the same time for concrete properties evaluation with incorporation NDT errors. This approach can be also adapted for concrete strength evaluation for existing concrete structures as buildings, bridges, etc. Additional studies are currently conducted in order to study the effect of complementary parameters such as concrete variability, the number of cores, the autocorrelation length, the marginal distribution function, the autocorrelation function on the efficiency of the developed methodology. Tests on real cases are currently implemented for testing the efficiency of the developed approach.

## REFERENCES

- [1] Alwash M., Sbartai Z.M., Breysse D., "Non-destructive assessment of both mean strength and variability of concrete: a new bi-objective approach", *Constr. Build. Mater.*, Vol. 113, pp. 880-889 (2016).
- [2] Fiore A., Porco F., Uva G., Mezzina M., "On the dispersion of data collected by in situ diagnostic of the existing concrete", *Const. Build. Mat.*, Vol. 47, p. 208-217 (2013).
- [3] Uva G., Porco F., Fiore A., Mezzina M., "Proposal of a methodology for assessing the reliability of in situ concrete tests and improving the estimate of the compressive strength", *Const. Build. Mat.*, Vol. 38, p. 72-83 (2013).
- [4] Villain G., Sbartai Z. M., Dérobert X., Garnier V., Balayssac J.P., "Durability diagnosis of a concrete structure in a tidal zone by combining NDT methods: laboratory tests and case study", *Const. Build. Mat.*, Vol. 37, p.893–903 (2012).
- [5] Ali-Benyahia K., Sbartai Z.M., Breysse D., Kenai S., Ghrici M., "Analysis of the single and combined non-destructive test approaches for on-site concrete strength assessment: General statements based on a real case-study", *Cases Stud. in Constr. Mater.*, Vol. 16, p.109-119 (2017).
- [6] Schoefs F., Tran T.V. , Bastidas-Arteaga E., Villain G., Derobert X., O'Connor A.J., Bonnet S.,

“Optimization of non-destructive testing when assessing stationary stochastic processes: application to water and chloride content in concrete”, *ICDS12*, 15p. (2012).

[7] Vona M., Nigro D., “Evaluation of the predictive ability of the in-situ concrete strength through core drilling and its effects on the capacity of the RC columns”, *Mat. and Struct.*, Vol. 39, p. 149-160 (2013).

[8] Pucinotti R., “Reinforced concrete structure: Non-destructive in situ strength assessment of concrete”, *Const. Build. Mat.*, Vol. 75, p. 331-341 (2015).

[9] Balayssac J.P., Garnier V., Villain G., Sbartai M., Dérobert X., Piwakowski B., Breysse D., Salin J. “An overview of 15 years of French collaborative projects for the characterization of concrete properties by combining NDT methods”, *Proceedings of Int. Symp. on NDT-CE*, (2015).

[10] Montgomery D., Runger G., “Applied Statistics and Probability for Engineers”, 7<sup>th</sup> ed. , John Wiley & Sons Inc., 710p. (2018).

[11] Ross M.S., “Introduction to Probability and Statistics for Engineers and Scientists”, fourth ed., Elsevier Inc., 680p. (2009).

[12] DeCoursey W.J., “Statistics and Probability for Engineering Applications”, Elsevier Inc., 396p. (2003).

[13] EN 13791, “Assessment of In Situ Compressive Strength in Structures and Precast Concrete”, CEN, 28p. (2007).

[14] Kheder G.F., “A two stage procedure for assessment of in situ concrete strength using combined non-destructive testing”, *Mater. Struct.*, Vol. 32, p. 410–417 (1999).

[15] Knaze P., Beno P., “The use of combined non-destructive testing methods to determine the compressive strength of concrete”, *Mater. Constr.*, Vol. 17, Issue 99, p. 207–210 (1984).

[16] Garnier V., “Analyse et Capitalisation pour le Diagnostic des Constructions”, Rapport final, projet C2D2 – ACDC, 63p. (2014).

[17] Breysse D., Lataste J.F., Balayssac J.P., Garnier V., “Quality and accuracy of concrete assessment provided by NDT measurement”, *6th International Probabilistic Workshop*, (2008).

[18] Breysse D., “Nondestructive evaluation of concrete strength: An historical review and a new perspective by combining NDT methods”, *Constr. Build. Mater.*, Vol. 33, p.139-163 (2012).

[19] Tumidajski P.J., Schumacher A.S., Perron S., Gu P., Beaudoin J.J., “On the relationship between porosity and electrical resistivity in cementitious systems”, *Cement and Concrete Research*, Vol. 26, Issue 4, p. 539–544 (1996).

[20] Klysz G., Balayssac J.P., “Determination of volumetric water content of concrete using ground-penetrating radar”, *Cement and Concrete Research*, Vol. 37, Issue 8, p. 1164-1171 (2007).

- [21] Fares M., Villain G., Fargier Y., Thiery M., Dérobert X., Palma Lopes S., "Estimation of water gradient and concrete durability indicators using capacitive and electrical probes", *Proceedings of Int. Symp. on NDT-CE*, (2015).
- [22] Sbartai Z.M., Laurens S., Rhazi J., Balayssac J.P., Arliguie G., "Using radar direct wave for concrete condition assessment: Correlation with electrical resistivity", *Journal of Applied Geophysics*, Vol. 62, Issue 4, , p. 361-374 (2007).
- [23] Balayssac J.P., Laurens S., Arliguie G., Breyse D., Garnier V., Dérobert X., Piwakowski B., "Description of the general outlines of the French project SENSO – Quality assessment and limits of different NDT methods"», *Constr. Build. Mater.*, Vol. 35, p.131–138 (2012).
- [24] Abraham O., Métais V., Villain G., Plantier G., Le Duff A., Durand O., "Influence of water gradient on surface wave measurements in concrete", *Proceedings of Int. Symp. On NDT-CE*, (2015).
- [25] Wenpeng S. , Bangrang D. , Jianxin W., Qian L., "Experimental study of water saturation effect on acoustic velocity of sandstones ", *Jour. of Natu. Gas Science and Engi.*, Vol. 33, p. 37-43 (2016).
- [26] Soshiroda T., Voraputhaporn K., Nozaki Y., "Early-stage inspection of concrete quality in structures by combined non-destructive method", *Mat. and Struct.* , Vol. 39, p. 149-160 (2006).
- [27] Komlos K., Popovics S., Nurnbergerova T., Babal B., Popovics J.S., "Ultrasonic Pulse Velocity Test of Concrete Properties as Specified in Various Standards", *Cem. And Concr. Comp.*, Vol. 18, p. 357-364 (1996).
- [28] Alwash M., Breyse D., Sbartai, ZM., " Non-destructive strength evaluation of concrete: Analysis of some key factors using synthetic simulations", *Constr. Build. Mater.*, Vol. 99, p. 235-245 (2015).
- [29] Breyse D., Klysz G., Dérobert X., Sirieix C., Lataste J.F., "How to combine several nondestructive techniques for a better assessment of concrete structures", *Cem. Con. Res.*, Vol. 38, p. 783-793 (2008).
- [30] Stewart M.G., Suo Q., "Extent of spatially variable corrosion damage as an indicator of strength and time-dependent reliability of RC beams", *Engineering Structures*, Vol. 31, p.198-207 (2009).
- [31] Nguyen N. T., Sbartai Z.M., Lataste J.F., Breyse D., Bos F., "Assessing the spatial variability of concrete structures using NDT techniques: Laboratory tests and case study", *Const. Build. Mater.*, Vol. 49, p. 240-250 (2013).
- [32] Gomez-Cardenas C., Sbartai Z.M., Balayssac J.P., Garnier V., Breyse D. , "New optimisation algorithm for optimal spatial sampling during non-destructive testing of concrete structures", *Eng. Struct.*, Vol. 88, p. 92-99 (2015).
- [33] Nguyen N. T., Sbartai Z.M., Lataste J.F., Breyse D., Bos F., " Non-destructive evaluation of the spatial variability of reinforced concrete structure", *21ème Congrès Français de Mécanique*, Vol. 16, Issue 1, 6p (2015).

- [34] Tsui F., Matthews S. L., "Analytical Modelling of The Dielectric properties of concrete For Subsurface Radar Applications", *Constr. Build. Mater.*, Vol. 11, Issue 3, pp. 149-161 (1997).
- [35] Laurens S., El Barrak M., Balayssac J.P., Rhazi J., "Aptitude of the near-field direct wave on radar ground-coupled antennas for the characterisation of the covercrete", *Constr. Build. Mater.*, Vol. 21, Issue 12, p.2072–2077 (2007).
- [36] Dérobert X., Iaquina J., Klysz G., Balayssac J.P., "Use of capacitive and GPR techniques for the non-destructive evaluation of cover concrete", *NDT & E Int.*, Vol. 41, Issue 1, p. 44–52. (2008).
- [37] Archie G., "The electrical resistivity log as an aid in determining some reservoir Characteristics", *Transaction of the American Institute of Mining and Metallurgical Engineers*, Vol. 146, Issue 1, p. 54–62 (1942).
- [38] Sleiman R. G., Panagiotis P., Michael M.G., Ben A. S. , "Measurement of ultrasonic phase and group velocities in human dental hard tissue", *J. Ther. Ultrasound*, Vol. 1, Issue 5, 10p. (2013).
- [39] Allan J. Z., "Handbook of the Speed of Sound in Real Gases: Speed of Sound in Air-volume 3", 1<sup>st</sup> ed., *Elsevier*, 301p. (2002).
- [40] Bonnans J.F., Gilbert J.C., Lemarechal C., Sagastizábal C.A., "Numerical Optimization", *Springer*, (2006).
- [41] Breyse D et al., "Recommendation of RILEM TC249-ISC on non destructive in situ strength assessment of concrete" ., *Materials and Structures* (2019)52:71.